Impact from Climate Change on extreme winds and icing conditions in the Baltic Region

Niels-Erik Clausen[1], Sven-Erik Gryning[1], Xiaoli Guo Larsén[1], Niels Jacob Tarp-Johansen[1], Hannele Holttinen[3], Rebecca Barthelmie[1], Sara Pryor[1,2] ,Per Lundsager[1]

[1]Risoe National Laboratory, Roskilde, Denmark, [2]Indiana University, Bloomington, USA, [3]VTT, Espoo, Finland,

SUMMARY The work presented is part of the Climate and Energy (CE) project 2003-2006. This paper describes the achievements in the wind energy work package dealing with the assessment of changes of average and extreme wind conditions as well as icing conditions in the Baltic Sea. The climate changes are analysed through scenarios generated by the regional atmosphere-ocean model RCAO of the SMHI Rossby Centre. In this paper the IPCC climate scenario A2 is considered with two sets of boundary conditions set by two General Circulation Models (GCMs) developed by the Max Planck Institute and the Hadley Centre respectively. An increase in the mean wind speed and the 50-year extreme wind is found as well as a decrease in ice cover both in terms of duration and geographical coverage. The impact on wind turbine design criteria is low and the analysis suggests that today's design criteria are applicable.

Keywords: Climate change, wind energy, extreme wind, ice, Baltic Sea

Background and context

For production of electricity in the Nordic countries renewable energy contribute by some 99% in Norway (hydro); 40-50% in Sweden (hydro); 30-40% in Finland (10%-20% from hydro and 20% based on biomass), 17% in Denmark (wind, increased to 20% in 2003), and 80% for Iceland is from hydro and 20% from geothermal. Figures are from 2001 [1].

The total installed offshore wind energy capacity in the Nordic countries is 423 MW of which 400 MW is located in Danish waters and 23 MW in Swedish territory. Large projects are planned in the Baltic Sea for the German, the Swedish and the Danish part to be implemented in the near future. Today offshore wind energy constitutes approximately 2.5% of the installed global capacity. According to the forecast from BTM Consult [2] the share from offshore will increase to some 7% in 2009.

The aim of the Climate & Energy project (CE) www.os.is/ce is an assessment of the impact of climate change on renewable energy resources in the Nordic region including hydropower, wind power, bio-fuels and solar energy. In the following we will deal only with the work related to assessment of climate impact on the offshore wind energy in the Baltic Sea.

Changes in the climate might bring changes to the average wind conditions. This is reported previously [3, 4]. Below we will investigate possible changes in extreme winds and icing conditions in the Baltic area.

The analysis is based on regional simulations conducted for the PRUDENCE project [5] by SMHI using the Rossby Centre coupled regional climate model (RCAO) [6]. Boundary conditions for the simulations were derived from two General Circulation Models (GCMs):

- The ECHAM4/OPYC3 [7] coupled Atmosphere-Ocean GCM developed by the Max Planck Institute, Hamburg and called MPI in the following (spectral resolution $\approx$ 2.8º x 2.8º).
- HadAM3H [8] atmosphere-only GCM developed at the Hadley Centre and called in the following HC; (Cartesian model with resolution 1.875º longitude x 1.25º latitude) with prescribed sea surface temperatures and ice coverage.

The RCAO model was run on a rotated longitude-latitude grid with 0.44x0.44º resolution (106 x 102 grid boxes) covering a domain which extended from 3.5°E, 51°N (lower left corner) to 38°E 72°N (upper right corner). The atmospheric component of the model had 24 levels in the vertical direction. The ocean model was run with 11 km horizontal resolution and 41 levels. Here we use 4-times daily output from the

RCAO (u and v components of the flow at 10-m) at two spatial resolutions (the rotated 0.44ºx0.44º simulation grid and an interpolated 0.5ºx0.5º resolution grid), for the two GCM lateral boundary conditions and two scenarios:

- Control run: January 1961 - December 1990
- A2 scenario: January 2071 - December 2100

Formateret: Punktopstilling

The emission scenario A2 used for the projected simulations are taken from those developed under the auspices of the IPCC [9]. The A2 scenario equates to a moderate to high greenhouse gas cumulative emission for 1990 to 2100, as a result of projected population growth and fairly slow introduction of alternative technologies. This scenario results in global carbon dioxide (CO_2) emissions from industry and energy in 2100 that are almost four times the year-1900 value.

Additionally the NCEP/NCAR (NNR) reanalysis data were applied. These data are available on a very coarse grid (1.875°x1.904°) and are therefore not directly comparable to data from RCAO simulations.

A parallel empirical downscaling has been developed [11] and in [12] in addition to the analysis of the RCAO model output to derive dynamically downscaled assessments of mean and extreme wind speeds and energy density at the end of the 21st century relative to the end of the 20th century. The parallel approach was applied to the Baltic region in [11] and [12]. Application of a range of downscaling techniques to a variety of Atmospheric, Ocean General Circulation models (AOGCM) is being used to provide a comprehensive assessment of the uncertainties in wind climate projections.

Extreme winds

We analyze the 50-year extreme wind U_{50} calculated from the 10 m horizontal winds in MPI (more specific) and HC, and their changes from the control run (1961 – 1990) to the A2 scenario (2071 – 2100). Additionally we discuss the distribution of U_{50} from the NCEP/NCAR reanalysis (NNR). The extreme wind here is calculated with the Annual Maximum Method as described in [13] and [14] Thus, 30 annual wind maxima are selected and sorted in ascending order. The distribution of the sorted wind maxima is then approximated by the double exponential, i.e. Gumbel, distribution.

The extreme winds at each grid points are shown in Figure 1, for MPI and HC, for the control run and A2 scenario. The general pattern is that the winds are higher over water, with clear hotspots in the Atlantic and the Baltic Sea, while over land it is quite low. For MPI, the hotspots in the Atlantic are larger than 27 ms^{-1} in the control run and 29 ms^{-1} in A2. Those in the Baltic Sea are about 23 ms^{-1} in the control run and 23 – 26 ms^{-1} in A2. For HC, the hotspots in the Atlantic are slightly larger than 29 ms^{-1} in the control run and the same order in A2, but in the Baltic Sea they are only about 21 ms^{-1} in the control run and 22 – 25 ms^{-1} in A2.
For HC, there is a distinct hotspot of 29 ms^{-1} in the west coast of Norway, centred at around (61N, 3E), both in the control run and A2; this is not found in MPI. This is, however, different from the results of NNR, which indicates a general and gradual decrease in U_{50} from the west to the east in the domain of the Atlantic, see Figure 2.

The comparison between the two models (Figure 3) for the control run shows that HC provides ~ 5 – 10% higher values than MPI from the northwest corner to the southern coast of Norway, and 10 – 15% lower values over middle-south part of Denmark and northern Germany. In A2, the difference in the southern part is small but reaches 12% over quite a large part of the land around the Baltic Sea.
Due to the crude spatial resolution of NNR (1.875°×1.904°), the contour lines in Figure 2 do not form the coastlines as clearly as those of MPI and HC. NNR has contour lines of the greatest gradients along the coastlines over land while MPI and HC have them over water. In Figure 4 all U_{50} values of MPI and HC within the area of four neighbouring NNR grids are averaged and compared with the NNR-U_{50} at the centre of the area. In both cases, the largest discrepancies to NNR are along the coast, with NNR having larger values of approximately 10 – 50%, corresponding to 2 – 8 ms^{-1}.
The ranges and the mean values of U_{50} from MPI, HC and NNR are provided in Table 1, from which one can also see the increase in MPI, A2 compared with the control run, and the only slight change in HC. NNR has larger mean value than the control runs of MPI and HC.

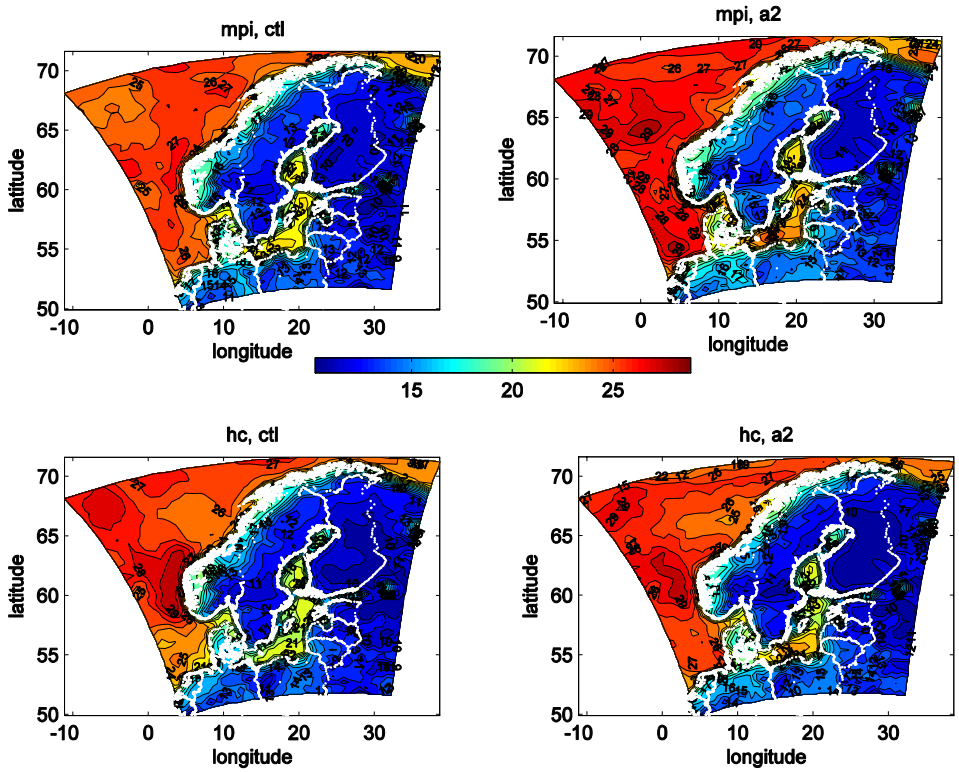

Figure 1: Spatial distribution of U_{50} (ms^{-1}) from MPI, control run and A2 scenario (upper panels), and from HC (lower panels).

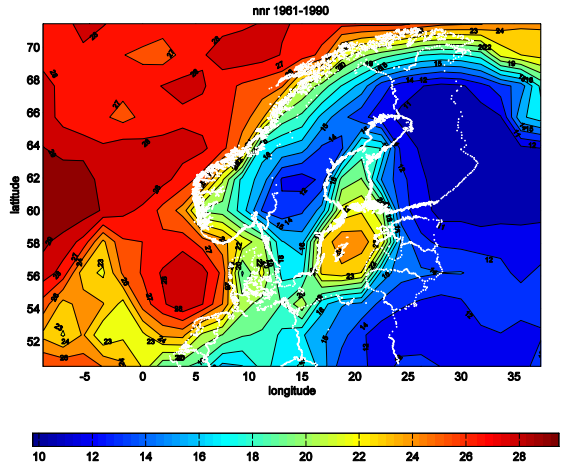

Figure 2: Spatial distribution of U_{50} from the NCEP/NCAR reanalysis data of the same period as MPI and HC.

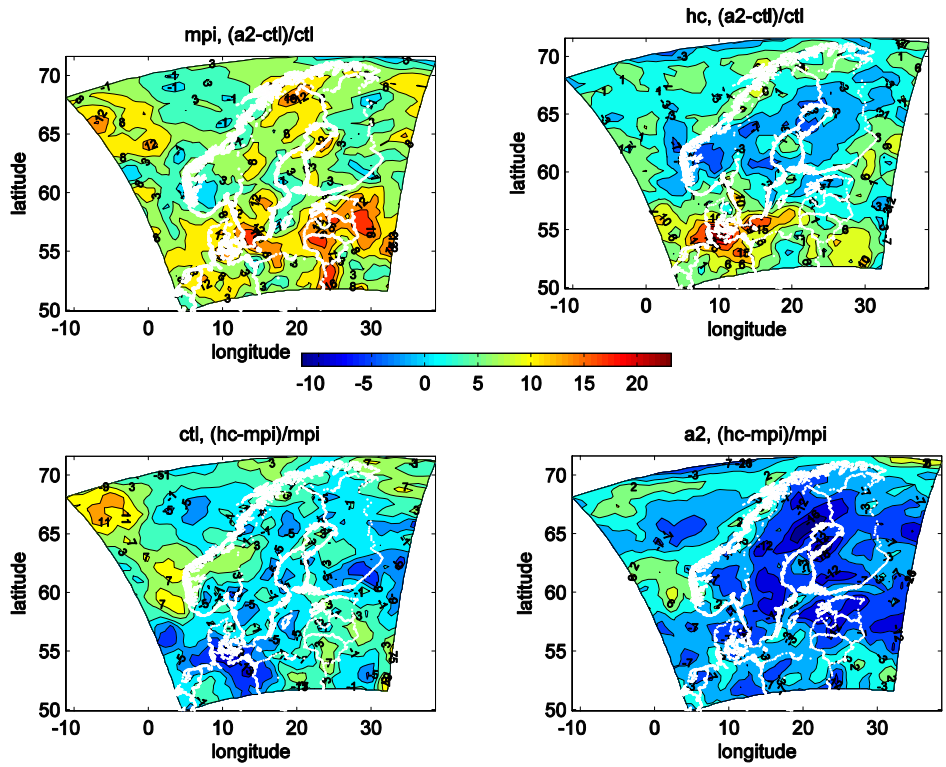

Figure 3: Relative differences of U50 in per cent between the control run and A2 scenario in MPI and HC (upper panels), and the differences between the two models for the control run and A2 scenario respectively (lower panels).

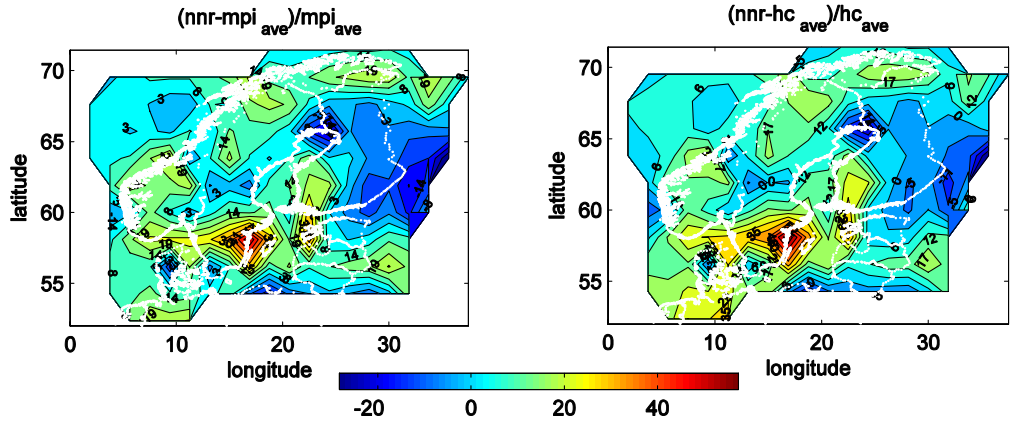

Figure 4: Relative differences in U_{50} in percent between MPI and NNR (left), and between HC and NNR (right).

		Range (ms^{-1})	Mean (ms^{-1})
MPI	Control period	9.45 – 28.00	17.98
	A2 scenario	10.22 – 29.74	19.04
HC	Control period	9.50 – 29.58	17.86
	A2 scenario	9.51 – 29.42	18.10
NNR	1961-1990	9.76 – 30.79	20.69

Table 1: Range and the mean value of the 50-year wind over the domain in MPI, HC and NNR.

Change in average wind speed

The percent wise change in the average wind speed is presented in Figure 5. For the simulations carried out with the MPI model, a marked increase in the average wind speed for the A2 scenario can be observed as compared to the control run, being up to 15% in the Northern part of the Baltic Sea and along the coast of Norway. Interesting enough the clear overall increase in the wind speed that is found in the MPI simulations is not found in the simulations with the HC model, where the change in the wind climate for the control run to the A2 scenario is smaller and often negative, but with the larger increase in wind speed found in the Baltic Sea. Therefore both model simulations suggest changes to the average wind climate over the Baltic Sea in such a way that the wind increases as compared to the control run. The middle panels illustrate that for the control run the average winds in the northern part of the modelling domain are higher in the simulations with the HC model that for MPI, and the tendency is reversed to the south. The data from NNR are only for the control run period. The lower panels shows that the average wind for NNR simulations are generally higher in the Baltic Sea as in the control runs.

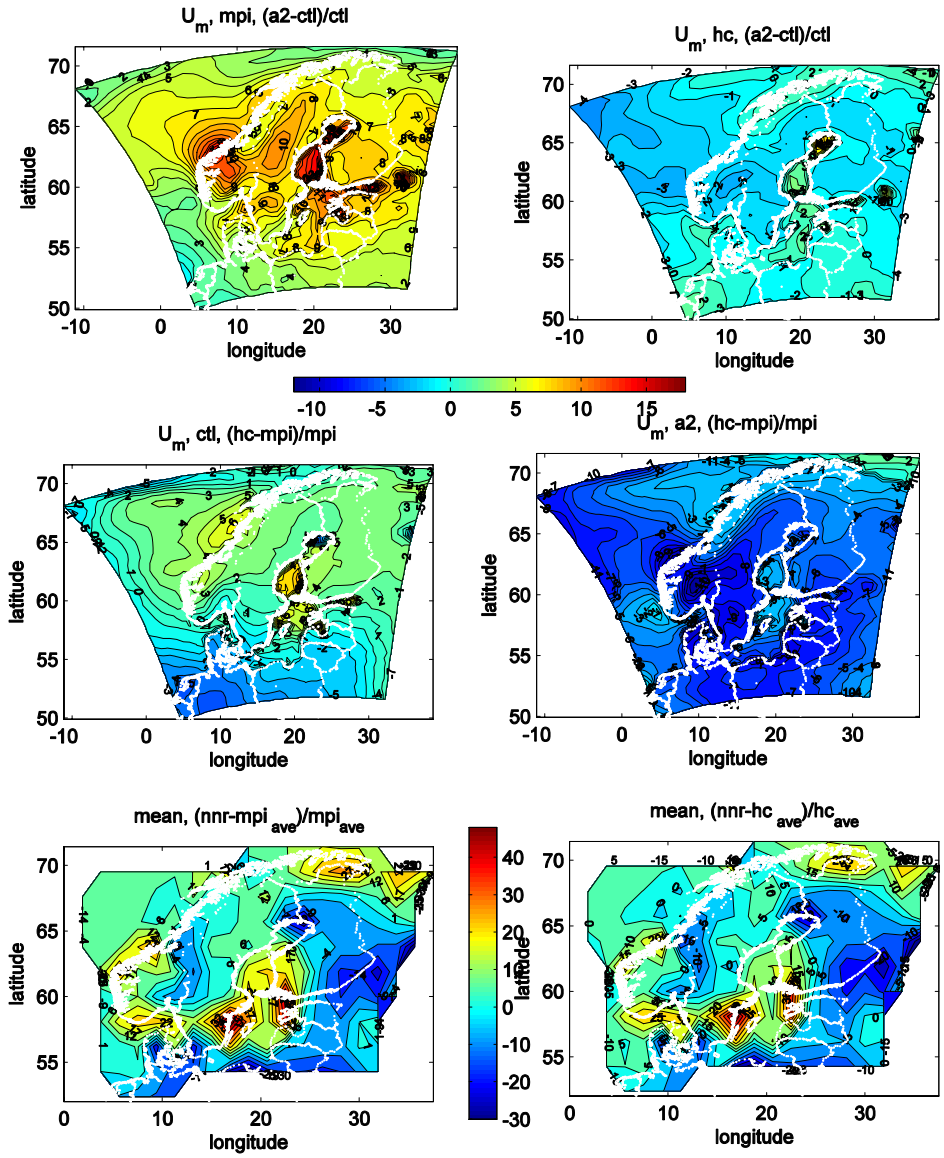

Figure 5: Relative difference in percent of the average wind speed for the MPI, HC and NNR model simulations.

Impact on design of offshore wind turbines

Wind turbines are mass-produced rather than designed for specific sites. Therefore design of wind turbines is made according to classification standards that define a number of so-called wind classes. Whenever a site has been chosen for the erection of turbines the wind climate at that site must be evaluated and a suitable wind class that covers this climate will be determined. At least this is the case for onshore turbines. Offshore turbines are often built in larger farms. For this reason site-specific design of the support structure, including the tower may be economically feasible, whereas the rotor-nacelle-assembly would still be mass-produced. Thus, when evaluating the possible impact of the wind climate change on the design of offshore wind turbines, one would have to look both at the change relative to the wind classes, and the change in loads as they may be derived from the wind climate change at the specific site regarded.

In this section the impact of the climate change on the design of offshore wind turbines is discussed with focus on the wind generated loads. The discussion is based on a single example considering a generic 2 MW turbine at a specific site in the Baltic Sea. As can be seen from figure Figure 3 offshore sites in the Baltic Sea experience the larger changes in the extreme wind climate and consequently the highest impact. Here we concentrate the study of impact on an offshore site located east of the island of Bornholm in the Baltic Sea. The modelled wind speed at 10 m height was extrapolated to hub height (80 m) by use of standard surface layer scaling. From this time series (data 4 times daily) U_{50} and average wind speeds at hub height was estimated.

With reference to the IEC standard 61400-1 Ed. 2 'WIND TURBINES: Design requirements' the wind climate at the selected site is considered. The standard classifies the wind climate according to the conditions at hub-height. There are 8 standard classes and a class 'special'. The standard classes are characterised by the 50-yr extreme wind speed U_{50} (in the IEC standard V_{ref}), the annual mean wind speed U_m (in the IEC standard V_{ave}), and the turbulence intensity (I). For instance class I_A has U_{50} = 50 m/s and U_m = 10 m/s, and class III_A has U_{50} = 37.5 m/s and U_m = 7.5 m/s. In this study a hub height of 80 m, typical of a 2 MW turbine, has been considered. Comparing the 50-yr extreme wind speeds and the mean wind speeds derived from the analysis of the 80m wind in the four different situations to the class definitions, it turns out that with respect to 50-yr extreme wind speeds class III_A is in all four situations the minimum class that covers this site, whereas for mean wind speeds the more severe class I_A is, also for all for situations, the minimum class. Thus in all four situations the minimum class is the same, namely I_A. So, from a classification point of view the wind climate change has no impact. The reason why the extreme winds fit into one class and the mean winds fit into another class is that IEC standard defines the ratio of U_{50} / U_m to be 5. This is a feature that many sites satisfy, but not for this site, neither for the control period, nor for the projected period. In the present case the ratio between extreme and average wind is about 3.5.

Finally we investigate the impact of changes in extreme wind conditions on site-specific design. Extreme loads generated by the 50-yr wind conditions and fatigue loads derived from the fitted Weibull distributions were considered. No wave loading was included. Only two load cases have been considered: normal operation and extreme wind situation. No detailed investigation of yaw misalignment, start-up, shut-down, or extreme gusts have been included, which compares well to the overall accuracy of the climate scenarios for 2071-2100. The flap and edge blade root moments plus the overturning moment and base shear are calculated, as they will be clearly representative of the major trends in the impact on design. It is noted that the turbulence intensities used in the response calculations have been estimated from measurements taken from other sites, as turbulence intensities have not been made available. The HC model gives rise to at most 1.5% change in fatigue loads, which is insignificant. The MPI gives rise to 2.5-5.0% increase in fatigue, which is not drastic. It is within the uncertainty of the load model and response models, but of course it agrees with the trends seen in the wind climate change. The change in extreme loads is for both models an increase of about 15%, which is sufficient to change the design of some parts of offshore turbines. Depending on the wind turbine manufacturer the design of the support structure is either fatigue or extreme load driven, so nothing can be said in general. At last it is noted that if one adds to the extreme wind loads the associated extreme wave loads that, dependent on the site-specific bottom topography, will increase with the extreme wind the extreme loads can become

significant for the design of the substructure and foundation, i.e. all parts of the support structure below mean water level.

Sea Ice and Icing in the Baltic

For offshore wind farms, ice cover of the sea may affect the design of turbine foundations. Atmospheric icing may affect also wind turbines, most critically the efficiency and lifetime of turbines blades. The analyses made so far indicate that the main impact of climate change will be to reduce the area of sea ice cover in the Baltic Sea and the number of icing events.

Sea Ice

Today, the sea will ice up every year in the Northern part of Baltic Sea. In Gulf of Bothnia North, the icing period in winter lasts on average 150-200 days: ice starts to form in the Northern part of the Gulf of Bothnia in November, the entire sea area is frozen by mid January, and the ice melts during May. The thickness of ice varies between 50 - 70 cm during normal winters and 80 - 110 cm during colder winters [15]. In the coastal areas of Gulf of Bothnia South and Gulf of Finland icing period lasts on average 100-150 days. South of Stockholm icing period is on average less than 60 days. In the sea areas around Denmark and West/South coast of Sweden the icing period is less than 30 days on average.

For wind turbine foundations, the most critical issue is the thickness of moving ice. In coastal regions limited ice action is exerted against the foundations, as the ice becomes anchored on the shoreline, rocks, shallows and islands. Early in the winter ice movements are by thin ice only, while during late spring the ice becomes soft and deteriorated and movements by thick ice is seen. In the Northern part of the Baltic Sea, moving ice can be 0.8 m thick with significant piling of ice. During winter loads on structures are from thermal ice expansion only. After a storm, ice floes that have broken off can move about causing loading on structures. The larger the solid ice field the larger the loads [16]. The greatest loads are usually experienced in springtime, when ice starts moving and piling. In the Northern part of Baltic Sea, the pile up against the tower and foundation can reach a height of ten meters and damage tower structures.

The climate model runs were analysed for sea ice. The grid size is about 49 km in RCAO model, but the ocean model for Baltic Sea (RCO) is more detailed with 11 km grid. The sea ice conditions in the regional model used in the climate runs are described in [17].

The climate scenario results are in these figures from A2 scenario, global model HC model, regional model RCAO. As the climate change might result in increased temperatures, the area with ice cover will decrease. According to the climate model run results, the length of average year icing period will diminish to about half in 100 years (Figure 6). On average, long icing periods (>100 days) would occur only in the Gulf of Bothnia, North. and in the Gulf of Finland. As there is considerable difference in coldest and mildest winters, also the maximum length of icing period was looked at (Figure 7). Today, in cold winters the whole of the Baltic Sea can ice up. The length of icing period can be more than 200 days in the Northern coast of Finland, more than 100 days along the East coast of Sweden and between Zealand and Jutland. In 2070-2100, it is anticipated that even during coldest winters the length of icing period will be less than 30 days on some coastal areas South of Stockholm and most of the Southern part of Baltic Sea will not ice up. What is now considered an average length of icing period would only occur during the coldest winters.

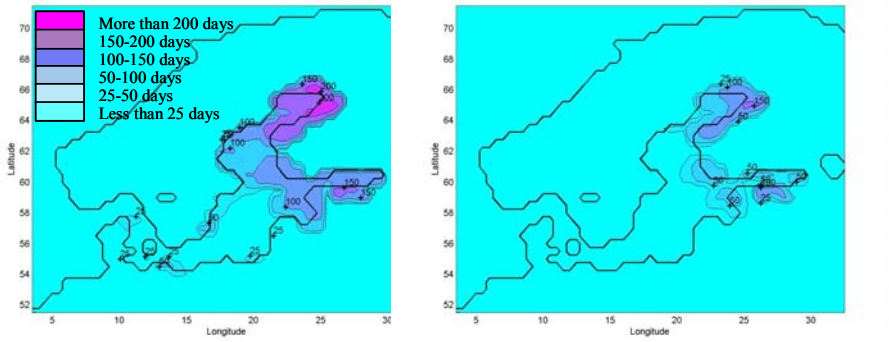

Figure 6. Average length of icing period, in days, for Baltic sea, during reference period 1960-90 (left) and during future scenario 2070-2100, scenario A2 (right). Model HC/RCAO. Average length of icing period for 30 years is calculated separately for each grid point.

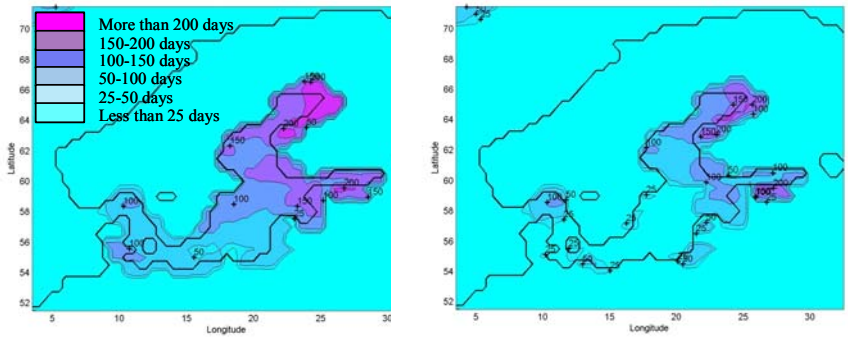

Figure 7. Maximum length of icing period, in days, for Baltic Sea, during reference period 1960-90 (left) and during future scenario 2070-2100, scenario A2 (right). Model HC/RCAO. 30 year maximum for each grid point is calculated separately.

As we are interested in design loads for wind turbines, the maximum ice fraction during 30 years period was also analysed. The maximum ice cover during February is presented in Figure 8 for reference scenario and for climate scenario 2070-2100. The figure shows the maximum ice fraction during February (in 30 years) for each point so it is not necessarily a simultaneous situation.

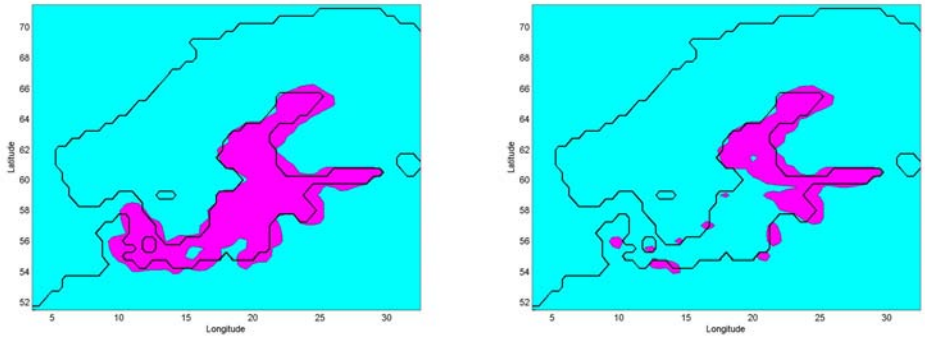

Figure 8. Area where maximum ice fraction in February has been > 0 during reference period 1960-90 (left) and during years 2070-2100, scenario A2 (right). Model HC/RCAO.

The data analysed include neither the thickness of ice, nor the thickness of moving ice that is critical design parameter for turbine foundations and towers. However, the reduced area where icing will occur will give some insight on the areas where ice loads due to sea ice should be taken into account in the future.

Atmospheric icing

Even a slight layer of ice on the blade can spoil the aerodynamics and cause production losses. Heavy icing can stop the turbine. Most of the time icing results in imbalance of the rotor and this can lead to considerable extra loads even at moderate icing accretions [18].

For wind turbines, it is necessary to estimate the total cumulative icing time, not just the time when ice formation will happen. Further estimation of production losses due to icing and the reduction of lifetime due to unbalanced loads is needed to determine whether blade heating or modified controls of turbines are needed.

It is difficult to determine when the meteorological conditions lead to icing. This is because icing is a local phenomenon and special ice detectors are scarce and not 100 % reliable. Icing can occur also when humidity sensors indicate less than 100 % humidity. Information on the height of cloud base and the type of rain (freezing rain) are used as indicators of icing events as well. Existing icing maps are based on meteorological weather stations data. Data periods and geographical coverage is limited especially at high levels above ground, relevant to wind turbines [19].

The first model result data was acquired for 60-80 m.a.g.l model level. For modern (2005) utility grade wind turbines this is lower than wind turbine hub height or blade tip in highest position. In the model there were no clouds forming this low, so the only indication of icing was made from combining temperature and humidity (frost point). According to model results icing at 60-80 m.a.g.l is now occurring in most parts of Finland (except southern coast), in many parts of Norway (except coastal sites) and in Northern parts of Sweden (North of Stockholm). Icing events occur mainly in January and February, little less in December and slightly in November and March. As time below 0°C will decrease remarkably due to climate change, also the time of icing events will decrease in the future. The southern parts of Nordic countries will not experience atmospheric icing near sea level. In 2071-2100, icing at 60-80 level above ground will occur in the northern parts of Finland, Sweden and Norway, and also in mountains in South Norway. Icing will only occur in January and February. However, the icing intensity and in-cloud icing for large turbines blade tip about 150 m.a.g.l is still unresolved.

Conclusions

Both climate models predict an increase in the extreme winds in the Baltic Sea of up to 15%. The average spatial increase is largest for MPI, but the Hadley scenario contains also an area across Denmark and south of Sweden with predicted increases in the extreme wind speeds in the 10-15% range. The average wind speed prediction for A2 scenario is a slight increase for MPI, while HC remains about the same.

The A2 scenario as modelled by the Hadley model predicts less icing in the Baltic Sea both in terms of days and in terms of geographical coverage. For the design of wind turbines no influence was found on design for fatigue. With increases in the 10-15% range of extreme winds the design for extreme loads is likely to be affected for some parts of a wind turbine.

References

[1] CIA World Factbook. *www.indexmundi.com*, 20 November 2004.

[2] BTM consult, *World market update,* March 2005.

[3] Clausen, N-E et.al., *Impact from climate change on the wind energy potential in the Nordic region*, in proceedings of European Wind Energy Conference, London 22-25 November 2004.

[4] Pryor, S.C. and R.J. Barthelmie, *Use of RCM simulations to assess the impact of climate change on wind energy availability*. 2004, Risoe National Laboratory: Roskilde, Denmark. p. 111 pp, RISO-R-1477, ISBN: 0106-2840 (available from: www.risoe.dk/rispubl/VEA/veapdf/ris-r-1477.pdf).

[5] Raisanen, J., et al., *European climate in the late twenty-first century: regional simulations with two driving global models and two forcing scenarios.* Climate Dynamics, 2004. **22**: p. 13-31.
[6] Raisanen, J., et al., *GCM driven simulations of recent and future climate with the Rossby Centre coupled atmosphere-Baltic Sea regional climate model RCAO*. 2003, Rossby Centre: SMHI, Norrkoping. p. 61 pp.
[7] Roeckner, E., et al., *Transient climate change simulations with a coupled atmosphere-ocean GCM including the tropospheric sulfur cycle.* Journal of Climate, 1999. **12**: p. 3004-3032.
[8] Pope, V., et al., *The impact of new physical parameterizations in the Hadley Centre climate model: HadAM3.* Climate Dynamics, 2000. **16**: p. 123-146
[9] IPCC, *Emissions Scenarios. 2000*, ed. N. Nakicenovic and R. Swart. 2000: Cambridge University Press, UK. 570.
[10] Pryor S.C., Barthelmie R.J., Kjellström E.: 2005a, 'Analyses of the potential climate change impact on wind energy resources in northern Europe using output from a Regional Climate Model', *Climate Dynamics* **In press**.
[11] Pryor S.C., Schoof J.T., Barthelmie R.J.: 2005b, 'Empirical downscaling of wind speed probability distributions', *Journal of Geophysical Research* **In press**.
[12] Pryor S.C., Schoof J.T., Barthelmie R.J.: 2005c, 'Potential climate change impacts on wind speeds and wind energy density in northern Europe: Results from empirical downscaling of multiple AOGCMs', *Climate Research* **In press**.
[13] Abild J., 1994: Application of the wind atlas method to extremes of wind climatology, Technical Report R-722(EN), Risø National Laboratory.
[14] Mann J., Kristensen L. and Jensen N.O., 1998: Uncertainties of extreme winds, spectra and coherences, Bridge Aerodynamics, Larsen & Eddahl (eds), Balkema, Rotterdam, ISBN 9054109610.
[15] Leppäranta, M., Palosuo, E., Grönvall, H., Kalliosaari, S., Seinä, A. and Peltola, J. Phases of the ice season in the Baltic Sea. 1988, Finnish Marine Research N:o 254, Supplement 2.
[16] Holttinen, H., Määttänen, M., Holttinen, E., Haapanen, E.. Offshore wind power in the ice infested waters of Gulf of Bothnia. Proceedings of European Wind Energy Conference EWEC'99. Based on report Offshore-tuulivoima Perämeren jääolosuhteissa. VTT Publications 828, Espoo, Finland 1998. 118 p. (in Finnish).
[17] Meier, M., Döscher, R. and Halkka, A. Simulated Distributions of Baltic Sea-ice in Warming Climate and Consequences for the Winter Habitat of the Baltic Ringed Seal. Ambio Vol. 33 No. 4–5, June 2004.
[18] Laakso, T., Holttinen, H., Ronsten, G., Tallhaug, L., Horbaty, R., Baring-Gould, I., Lacroix, A., Peltola, E., Tammelin, B., State-of-the-art of wind energy in cold climates. 2005, http://arcticwind.vtt.fi /
[19] Tammelin, B., Säntti, K., Icing in Europe, Proceeding of the International Conference, Wind Energy Production in Cold Climate, BOREAS IV, held at Hetta, Finland, 31 March - 2 April 1998, Published by: Finnish Meteorological Institute. Available at http://arcticwind.vtt.fi /

Acknowledgements

The work presented in the present paper is part of the Climate and Energy (CE) project 2003-2006, which is co-funded by the Nordic Energy Research (NEFP) and the energy sector in the Nordic countries. The project is coordinated by the National Energy Agency of Iceland (Orkustofnun). The co-operation with the SMHI Rossby Centre, which has delivered the climate scenarios from their Regional Climate model, is greatly acknowledged. The work on extreme winds is furthermore supported by the EC "Wind Energy Assessment and Wind Engineering" (WINDENG) Training Network (contract n. HPRN-CT-2002-00215) and Danish Research Agency grant 2104-04-0005 "offshore wind power". The NCEP/NCAR reanalysis data are provided by the NOAA-CIRES Climate Diagnostics Centre, Boulder, Colorado, from their web site at http://www.cdc.noaa.gov/.

Abbreviations

AOGCM	Atmospheric, Ocean General Circulation Model
GCM	General Circulation Model
HC	Hadley Centre
IPCC	Intergovernmental Panel on Climate Change
MPI	Max Planck Institute
NCAR	National Centre of Atmospheric Research
NCEP	National Center of Environmental Prediction
NEFP	Nordic Energy Research Program
NNR	NCEP / NCAR Re-analysis data
RCAO	Rossby Centre regional coupled Atmosphere-Ocean model
RCM	Rossby Center Regional Climate model
SMHI	Swedish Meteorological and Hydrological Institute
SRES	IPCC Special Report on Emission Scenarios